

Improving LMA predictions with non standard interactions

C. R. Das*, João Pulido†

CENTRO DE FÍSICA TEÓRICA DAS PARTÍCULAS (CFTP)

Departamento de Física, Instituto Superior Técnico

Av. Rovisco Pais, P-1049-001 Lisboa, Portugal

Abstract

It has been known for some time that the well established LMA solution to the observed solar neutrino deficit fails to predict a flat energy spectrum for SuperKamiokande as opposed to what the data indicates. It also leads to a Chlorine rate which appears to be too high as compared to the data. We investigate the possible solution to these inconsistencies with non standard neutrino interactions, assuming that they come as extra contributions to the $\nu_\alpha\nu_\beta$ and $\nu_\alpha e$ vertices that affect both the propagation of neutrinos through solar matter and their detection. We find that, among the many possibilities for non standard couplings, only one of them leads to a flat SuperKamiokande spectral rate in better agreement with the data and predicts a Chlorine rate within 1σ of the observed one, while keeping all other predictions accurate.

*E-mail: crdas@cftp.ist.utl.pt

†E-mail: pulido@cftp.ist.utl.pt

1 Introduction

Neutrino non-standard interactions (NSI) have been introduced long ago [1, 2] to account for a possible alternative solution to the solar neutrino problem. Since then a great deal of effort has been dedicated to study its possible consequences. To this end possible NSI signatures in neutrino processes have been investigated, models for neutrino NSI have been developed and bounds have been derived [3, 4, 5, 6, 7, 8, 9, 10, 11, 12, 13, 14, 15, 16, 17]. Specific investigations of NSI in matter have also been performed within the context of supernova [18] and solar neutrinos [19, 20, 21, 22, 23, 24].

Although LMA is generally accepted as the dominant solution to the solar neutrino problem [25, 26], not only its robustness has been challenged by NSI, as it can shift the LMA solution to the dark side region of parameter space [22], but also some inconsistencies remain regarding its agreement with the data [27, 28]. In fact, while the SuperKamiokande (SK) energy spectrum appears to be flat [29, 30], the LMA prediction shows a clear negative slope in the same energy range. With the expected improvement in the trigger efficiency for threshold electron energies as low as 3 MeV to be reached in the near future [31], such a disagreement, if it persists, may become critical. Moreover the LMA solution predicts an event rate for the Cl experiment [32] which is 2σ above the observed one [33]. These are motivations to consider 'beyond LMA' solar neutrino solutions in which NSI may play a subdominant, although important role.

In order for NSI to be detectable and therefore relevant in physical processes, the characteristic scale of the new physics must not be too much higher than the scale of the physics giving rise to the Standard Model interactions, $\Lambda_{EW} \simeq G_F^{-1/2}$. Possible realisations are one loop radiative models of Majorana neutrino mass [34], supersymmetric SO(10) with broken D-parity [35], the inverse seesaw in a supersymmetry context [36] or triplet seesaw models [37]. Since the scale at which the new interaction arises is supposed to be not too far from the electroweak scale, its coupling may be parameterised by $G_F \varepsilon$ where $\varepsilon \simeq \Lambda_{EW}^2 / \Lambda_{NP}^2 \simeq 10^{-2}$ for d=6 or $\varepsilon \simeq \Lambda_{EW}^4 / \Lambda_{NP}^4 \simeq 10^{-4}$ for d=8 operators respectively. For type I seesaw, NSI are of course negligible.

In this paper we will be concerned with NSI both at the level of propagation through solar matter and at the level of detection. Matter NSI are defined through the addition of an effective operator to the Lagrangian density

$$\mathcal{L}_{NSI}^M = -2\sqrt{2}G_F\varepsilon_{\alpha\beta}^{fP}[\bar{f}\gamma^\mu P f][\bar{\nu}_\alpha\gamma_\mu P_L\nu_\beta] \quad (1)$$

where $f = e, u, d$, P denotes the projection operator for left and right chirality and $\varepsilon_{\alpha\beta}^{fP}$ parameterizes the deviation from the standard interactions. At present there is no evidence at all of such operators generated at a scale Λ_{NP} , hence the variety of theoretical models for the physics accessible to the LHC.

There are several ways to introduce NSI. For instance in fermionic seesaw models, once the heavy fermions (singlets or triplets) are integrated out, modified couplings of leptons to gauge bosons are obtained in the form of a non-unitary leptonic matrix. The strong bounds

on the deviation from the unitarity of this matrix constrain these NSI to be $\lesssim O(10^{-3})$ [13]. Alternatively NSI can be generated by other new physics above the electroweak scale not related to neutrino masses. As a consequence an $SU(2)$ gauge invariant formulation of NSI is required, since any gauge theory beyond the standard model must necessarily respect its gauge symmetry. Strong bounds from four charged fermionic processes [38] and electroweak precision tests requiring fine tunings imply that possibilities are limited for such scenarios [14, 39]. Another way to introduce NSI is by assuming that these are extra contributions to the vertices $\nu_\alpha\nu_\beta$ and $\nu_\alpha e$. In such a case the parameters $\varepsilon_{\alpha\beta}$ describe the deviation from the standard model vertices and are treated like the standard interactions. It is possible that other effects are present in this case that depend on the nature and number of particles that may be introduced in a particular model. We adopt this procedure in the present paper and assume these model dependent effects to be negligible.

The paper is organized as follows: section 2 is devoted to the study of the propagation and detection of solar neutrinos. We start by reviewing the derivation of the neutrino refraction indices with standard interactions (SI) and their generalization to NSI in order to obtain the matter Hamiltonian. The survival and conversion probabilities to ν_μ and ν_τ are then evaluated through the numerical integration of the Schrödinger like equation using the Runge-Kutta method and the experimental event rates are obtained. We use the reference solar model with high metallicity, BPS08(GS) [40]. In section 3 we investigate the influence of the NSI couplings on these rates in order to find whether and how the fits can be improved with respect to the LMA ones. We concentrate in particular on the elimination of the upturn in the SuperKamiokande spectrum predicted by LMA for energies below 8-10 MeV not supported by the data [27, 28, 29, 30] and on the Chlorine rate whose LMA prediction exceeds the data by 2σ [32, 33]. We find that there are quite limited possibilities for the NSI couplings allowing for such fit improvements. Finally in section 4 we draw our main conclusions.

2 Interaction potentials, the Hamiltonian and the rates

In this section we develop the framework that will be used as the starting point for the analysis of the NSI couplings in section 3. To this end we review the derivation of the neutrino interaction potentials in solar matter, its generalization to non standard interactions along with the corresponding matter Hamiltonian and the event rates.

2.1 Interaction potentials and the Hamiltonian

While ν_e 's propagate through solar matter their interaction with electrons proceeds both through charged and neutral currents (CC) and (NC). Recalling that for standard interac-

tions (SI) each tree level vertex accounts for a factor

$$\frac{g_L}{\cos\theta_W}(T_{3L} - 2Q_f \sin^2\theta_W), \quad (2)$$

inserting the W, Z propagators and the electron external lines, one gets for the ν_e interaction potentials

$$(V_e)_{CC} = G_F\sqrt{2}N_e, \quad (V_e)_{NC} = G_F/\sqrt{2}(-1 + 4\sin^2\theta_W)N_e \quad (3)$$

where G_F is the Fermi constant, $G_F/\sqrt{2} = g_L^2/8m_W^2$. For the interactions with quarks only neutral currents are involved and the additivity of the quark-current vertices gives for protons

$$V_p = (V_p)_{NC} = G_F/\sqrt{2}(1 - 4\sin^2\theta_W)N_e \quad (4)$$

and for neutrons

$$V_n = (V_n)_{NC} = -G_F/\sqrt{2}N_n. \quad (5)$$

Hence the neutrino interaction potential is for standard interactions [‡]

$$V(SI) = V_e + V_p + V_n = G\sqrt{2}N_e \left(1 - \frac{N_n}{2N_e}\right) = V_c + V_n \quad (6)$$

with $V_e = (V_e)_{CC} + (V_e)_{NC}$ and $V_c = V_e + V_p = G_F\sqrt{2}N_e$.

In order to introduce NSI we assume that each diagram associated to neutrino propagation in matter (i.e. CC and NC currents in $\nu_\alpha e^-$ and NC currents in $\nu_\alpha u, \nu_\alpha d$ scattering) is multiplied by a factor $\varepsilon_{\alpha\beta}^{e,u,d P}$ parameterising the deviation from the standard model. So we assume that the interaction potential for ν_α ($\alpha = e, \mu, \tau$) on electrons involves both CC and NC giving rise to possible lepton flavour violation: ν_α for $\alpha \neq e$ may have CC. So for the charged current of ν_e with electrons we have

$$(V_e)_{CC}(NSI) = \frac{g_L^2}{2m_W^2}(\varepsilon_{\alpha\beta}^{eP})_{CC}N_e \quad (7)$$

and for the neutral current

$$(V_e)_{NC}(NSI) = \frac{g_L^2}{4m_W^2}(-1 + 4\sin^2\theta_W)(\varepsilon_{\alpha\beta}^{eP})_{NC}N_e \quad (8)$$

where the NSI couplings affecting the CC and NC processes should in principle be distinguished.

Using equation (2) and the additivity of the quark-current vertices, one gets for the neutrino interaction potential with protons

$$V_p(NSI) = \frac{g_L^2}{2m_W^2} \left[\varepsilon_{\alpha\beta}^{uP} - \frac{\varepsilon_{\alpha\beta}^{dP}}{2} - \left(\frac{4}{3}2\varepsilon_{\alpha\beta}^{uP} - \frac{2}{3}2\varepsilon_{\alpha\beta}^{dP} \right) \sin^2\theta_W \right] N_e. \quad (9)$$

[‡]All expressions are divided by 2 to account for the fact that the medium is unpolarized.

Similarly for neutrons

$$V_n(NSI) = \frac{g_L^2}{2m_W^2} \left(\frac{\varepsilon_{\alpha\beta}^{uP}}{2} - \varepsilon_{\alpha\beta}^{dP} \right) N_n. \quad (10)$$

In both (9) and (10) only neutral currents are involved.

Adding (7), (8), (9) and (10) and dividing by 2 one finally gets

$$\begin{aligned} V(NSI) = & G\sqrt{2}N_e \left[(\varepsilon_{\alpha\beta}^{eP})_{CC} + \left(-\frac{1}{2} + 2\sin^2\theta_W \right) (\varepsilon_{\alpha\beta}^{eP})_{NC} + \left(1 - \frac{8}{3}\sin^2\theta_W + \frac{N_n}{2N_e} \right) \varepsilon_{\alpha\beta}^{uP} \right. \\ & \left. + \left(-\frac{1}{2} + \frac{2}{3}\sin^2\theta_W - \frac{N_n}{N_e} \right) \varepsilon_{\alpha\beta}^{dP} \right] \end{aligned} \quad (11)$$

which reduces to eq.(6) in the absence of NSI.

In the case of the standard interactions, the interaction potentials for ν_e and ν_α constitute a diagonal matrix because they cannot be responsible for flavour change [eq.(6)]. This may occur as a consequence of the vacuum mixing angle (oscillations) [25, 26] or the magnetic moment for instance [27, 28]. On the other hand, in the case of NSI the interaction potentials [eq.(11)] constitute a full matrix in neutrino flavour space.

In order to obtain the matter Hamiltonian eqs.(6) and (11) must now be added. In the flavour basis this is

$$\mathcal{H}_M = V_c \begin{pmatrix} 1 & 0 & 0 \\ 0 & 0 & 0 \\ 0 & 0 & 0 \end{pmatrix} + \begin{pmatrix} v_{ee}(NSI) & v_{e\mu}(NSI) & v_{e\tau}(NSI) \\ v_{\mu e}(NSI) & v_{\mu\mu}(NSI) & v_{\mu\tau}(NSI) \\ v_{\tau e}(NSI) & v_{\tau\mu}(NSI) & v_{\tau\tau}(NSI) \end{pmatrix} \quad (12)$$

where in the first term, describing the standard interactions, the additive quantity V_n which is proportional to the identity, has been removed from the diagonal. In the second term $v_{\alpha\beta}$ ($\alpha, \beta = e, \mu, \tau$) denote the matrix elements of the interaction potential matrix (11). Finally in the mass basis

$$\mathcal{H} = \begin{pmatrix} 0 & 0 & 0 \\ 0 & \frac{\Delta m_{21}^2}{2E} & 0 \\ 0 & 0 & \frac{\Delta m_{31}^2}{2E} \end{pmatrix} + U^\dagger \mathcal{H}_M U \quad (13)$$

where U is the PMNS matrix [41] [§], E is the neutrino energy and $\Delta m_{ij}^2 = m_i^2 - m_j^2$ with m_i ($i = 1, 2, 3$) the neutrino mass. Upon insertion of this Hamiltonian expression in the neutrino evolution equation, the survival (P_{ee}) and conversion probabilities ($P_{e\mu}, P_{e\tau}$) are evaluated using the Runge-Kutta numerical integration.

[§]We use the standard parameterization [42] for the U matrix and the central value $\sin\theta_{13} = 0.13$ claimed in ref. [25].

2.2 Neutrino electron scattering detection rates

For the detection in SuperKamiokande and SNO through $\nu_\alpha e^- \rightarrow \nu_\beta e^-$ scattering, the NSI information comes in the probabilities and the cross section

$$\frac{d\sigma}{dT} = \frac{2G_F^2 m_e}{\pi} \left[\tilde{g}_L^2 + \tilde{g}_R^2 \left(1 - \frac{T}{E_\nu} \right)^2 - \tilde{g}_L \tilde{g}_R \frac{m_e T}{E_\nu^2} \right] \quad (14)$$

where $\tilde{g}_{L,R}$ are the $g_{L,R}$ couplings modified according to [11]

$$\begin{aligned} (\tilde{g}_{L,R})_{\nu_e}^2 &= |(g_{L,R})_{\nu_e} + \varepsilon_{ee}^{L,R}|^2 + |\varepsilon_{\mu e}^{L,R}|^2 + |\varepsilon_{\tau e}^{L,R}|^2 & \text{for } \nu_e e^- \rightarrow \nu_\alpha e^- \\ (\tilde{g}_{L,R})_{\nu_\mu}^2 &= |(g_{L,R})_{\nu_\mu} + \varepsilon_{\mu\mu}^{L,R}|^2 + |\varepsilon_{e\mu}^{L,R}|^2 + |\varepsilon_{\tau\mu}^{L,R}|^2 & \text{for } \nu_\mu e^- \rightarrow \nu_\alpha e^- \\ (\tilde{g}_{L,R})_{\nu_\tau}^2 &= |(g_{L,R})_{\nu_\tau} + \varepsilon_{\tau\tau}^{L,R}|^2 + |\varepsilon_{e\tau}^{L,R}|^2 + |\varepsilon_{\mu\tau}^{L,R}|^2 & \text{for } \nu_\tau e^- \rightarrow \nu_\alpha e^- . \end{aligned}$$

with $\alpha = e, \mu, \tau$.

For ν_e both charged and neutral currents are possible, so that

$$(g_L)_{\nu_e} = \frac{1}{2} + \sin^2 \theta_W, \quad (g_R)_{\nu_e} = \sin^2 \theta_W \quad (15)$$

whereas $\nu_{\mu,\tau}$ only interact through neutral currents, hence

$$(g_L)_{\nu_\mu, \nu_\tau} = -\frac{1}{2} + \sin^2 \theta_W, \quad (g_R)_{\nu_\mu, \nu_\tau} = \sin^2 \theta_W. \quad (16)$$

These expressions are then inserted in the spectral event rate

$$R_{SK,SNO}^{th}(E_e) = \frac{\int_{m_e}^{E'_{max}} dE'_e f(E'_e, E_e) \int_{E_m}^{E_M} dE \phi(E) \left[P_{ee}(E) \frac{d\sigma_e}{dT'} + P_{e\mu}(E) \frac{d\sigma_\mu}{dT'} + P_{e\tau}(E) \frac{d\sigma_\tau}{dT'} \right]}{\int_{m_e}^{E'_{max}} dE'_e f(E'_e, E_e) \int_{E_m}^{E_M} dE \phi(E) \frac{d\sigma_e}{dT'}} \quad (17)$$

which will be evaluated in the next section. Here $\phi(E)$ denotes the neutrino flux from Boron and hep neutrinos, $f(E'_e, E_e)$ is the energy resolution function for SuperKamiokande and SNO [43, 44] and the rest of the notation is standard.

Notice that whereas the Hamiltonian (13) is symmetric under the interchange

$$\varepsilon_{\alpha\beta}^L \leftrightarrow \varepsilon_{\alpha\beta}^R \quad \text{for } e, u, d$$

such is not the case for the detection process [see eq.(14)-(16)]. We finally note that at the detection level the NSI couplings $\varepsilon_{\alpha\beta}^{L,R}$ are considered separately, as clearly seen from eqs.(14), whereas at the level of propagation, since the diagrams involved in the interaction potentials add up, their sum should instead be considered.

3 NSI couplings, probabilities and spectra

We now perform an investigation of the effect of the NSI couplings $\varepsilon_{\alpha\beta}^{e,u,d} = |\varepsilon_{\alpha\beta}^{e,u,d}| e^{i\phi_{\alpha\beta}^{e,u,d}}$ on the neutrino probability and event rates. Our aim is to find those couplings which lead to a flat SuperKamiokande spectral rate, thus improving the fit with respect to its LMA prediction while keeping the quality of the other solar event rate fits. We first consider equal CC and NC couplings, namely $(\varepsilon_{\alpha\beta}^{eP})_{CC} = (\varepsilon_{\alpha\beta}^{eP})_{NC} = \varepsilon_{\alpha\beta}^{eP}$ and in a second stage $(\varepsilon_{\alpha\beta}^{eP})_{CC} \neq (\varepsilon_{\alpha\beta}^{eP})_{NC}$.

3.1 $(\varepsilon_{\alpha\beta}^{eP})_{CC} = (\varepsilon_{\alpha\beta}^{eP})_{NC} = \varepsilon_{\alpha\beta}^{eP}$

For the sake of clarity we will organize the NSI couplings in three matrices according to whether the charged fermion in the external line is e , u , d

$$\begin{pmatrix} \varepsilon_{ee}^{e,u,d P} & \varepsilon_{e\mu}^{e,u,d P} & \varepsilon_{e\tau}^{e,u,d P} \\ \varepsilon_{\mu e}^{*e,u,d P} & \varepsilon_{\mu\mu}^{e,u,d P} & \varepsilon_{\mu\tau}^{e,u,d P} \\ \varepsilon_{\tau e}^{*e,u,d P} & \varepsilon_{\tau\mu}^{*e,u,d P} & \varepsilon_{\tau\tau}^{e,u,d P} \end{pmatrix}. \quad (18)$$

Each set of three couplings $\varepsilon_{\alpha\beta}^{e,u,d P}$ enters in equation (11) in the entry $v_{\alpha\beta}$ of the interaction potential matrix. Altogether there are 18 couplings with 36 parameters: each matrix of the three in eq.(18) contains 6 independent entries, each with a modulus and a phase. We analyse one coupling at a time, by taking all others zero. We first consider the cases of purely real and imaginary couplings, hence 4 possibilities for each phase

$$\phi_{\alpha\beta}^{e,u,d} = 0, \pi/2, \pi, (3/2)\pi. \quad (19)$$

Motivated by the arguments expound in the introduction we investigate the parameter range $|\varepsilon_{\alpha\beta}| \in [5 \times 10^{-5}, 5 \times 10^{-2}]$. We find that

- Off diagonal entries $\varepsilon_{\alpha\beta}^{e,u,d P}$ ($\alpha \neq \beta$) which contain $3 \times 3 \times 4 = 36$ possibilities for moduli and phases do not induce any change in the LMA probability, nor any visible change in the rates, either if one or more at a time are inserted.
- Diagonal entries $\varepsilon_{\alpha\alpha}^{e,u,d P}$.
 - (a) Real couplings $\varepsilon_{\alpha\alpha}^{e,u,d P} = \pm |\varepsilon_{\alpha\alpha}^{e,u,d P}|$ ($3 \times 3 \times 2 = 18$ possibilities) do not change the LMA probability, hence the rates.
 - (b) Imaginary couplings $\varepsilon_{\alpha\alpha}^{e,u,d P} = \pm i |\varepsilon_{\alpha\alpha}^{e,u,d P}|$ ($3 \times 3 \times 2 = 18$ possibilities) lead to probabilities which diverge from P_{LMA} for all $|\varepsilon_{\alpha\alpha}| > 5 \times 10^{-5}$. According to the probability shape that is obtained, we group these cases in the following way

	1	2	3
A	$+i \varepsilon_{ee}^e P $	$+i \varepsilon_{\mu\mu}^e P $	$-i \varepsilon_{ee}^e P $
B	$+i \varepsilon_{ee}^u P $	$+i \varepsilon_{\mu\mu}^u P $	$-i \varepsilon_{ee}^u P $
C	$-i \varepsilon_{ee}^d P $	$-i \varepsilon_{\mu\mu}^d P $	$+i \varepsilon_{ee}^d P $
D	$-i \varepsilon_{\mu\mu}^e P $	$-i \varepsilon_{\tau\tau}^e P $	$+i \varepsilon_{\tau\tau}^e P $
E	$-i \varepsilon_{\mu\mu}^u P $	$-i \varepsilon_{\tau\tau}^u P $	$+i \varepsilon_{\tau\tau}^u P $
F	$+i \varepsilon_{\mu\mu}^d P $	$+i \varepsilon_{\tau\tau}^d P $	$-i \varepsilon_{\tau\tau}^d P $

Table I - The NSI couplings that modify the LMA probability .

All cases in the first column of table I along with D2, E2, F2 in the second column lead qualitatively to the same monotonically decreasing probability curve: a high probability ($P \geq P_{LMA}$) for low energy ($E \lesssim 3MeV$) and a low one ($P \leq P_{LMA}$) for intermediate and high energies. The curve becomes increasingly flat in this energy sector as $\varepsilon_{\alpha\alpha}$ increases, which is also reflected in the flatness of the SuperKamiokande spectral rate. However for cases A1, B1, C1 and D2, E2, F2 the probability gets too high for low energies so that the Ga [45, 46] rate fails to be conveniently fitted. The 'best' results in the sense that they lead to the most flat spectral rate which approaches the SuperKamiokande one and to a correct fit for Ga are obtained alternatively from cases D1, E1, or F1 for the following values

$$\begin{aligned}
-i|\varepsilon_{\mu\mu}^e P| &= -i 1.5 \times 10^{-3} \\
-i|\varepsilon_{\mu\mu}^u P| &= -i 2.5 \times 10^{-3} \\
+i|\varepsilon_{\mu\mu}^d P| &= +i 2.0 \times 10^{-3}.
\end{aligned} \tag{20}$$

For larger values of the NSI couplings the probability moves further away from its LMA profile so that the Ga rate becomes too high and the 8B one too low. In fig.1 we plot four survival probabilities: at the lowest energy and from bottom to top the first curve is the LMA one, the next corresponds to all cases in (20) and leads to the best fit of the four, the next one to the case $-i|\varepsilon_{\mu\mu}^e P| = -i 3 \times 10^{-3}$ and the top one to $+i|\varepsilon_{ee}^e P| = +i 5 \times 10^{-3}$. A comparison is shown in table II between the predictions and the quality of the fits obtained from LMA and the case $-i|\varepsilon_{\mu\mu}^e P| = -i 1.5 \times 10^{-3}$. In figs.2 and 3 we show the SuperKamiokande spectrum for LMA (upper curves) and for the first case in (20) (lower curves) superimposed on the data points taken respectively from refs. [29] and [30]. The improvement obtained through the NSI coupling is clearly visible. In fig.4 the two curves are superimposed on the SNO data points for electron scattering [47]. Here the data are also clearly consistent with a constant rate.

	Ga	Cl	SK	SNO _{NC}	SNO _{CC}	SNO _{ES}	χ_{rates}^2	$\chi_{SK_{sp}}^2$	χ_{SNO}^2	χ_{gl}^2
LMA	64.9	2.84	2.40	5.47	1.79	2.37	0.67	42.0	48.6	91.3
$-i \varepsilon_{\mu\mu}^e P $	69.7	2.74	2.23	5.47	1.68	2.26	0.11	40.3	45.0	85.4

Table II - Comparison between the LMA predictions for solar event rates and the NSI ones with $-i|\varepsilon_{\mu\mu}^e P| = -i 1.5 \times 10^{-3}$. For details of the χ^2 analysis see for instance [27].

The first set of cases in the second column of table I, namely A2, B2, C2, lead qualitatively to the inverse behaviour with energy of the LMA probability. As $|\varepsilon_{\alpha\alpha}|$ increases from its lower bound, one gets $P \leq P_{LMA}$ for low energies ($E \lesssim 2 - 3 \text{ MeV}$) and $P \geq P_{LMA}$ for intermediate and high energies, so that the fits worsen with respect to the LMA ones.

Finally all cases in the third column of table I, namely A3, B3, C3, D3, E3, F3 lead to probability curves which are totally unsuitable: they deviate drastically from both P_{LMA} and a from flat, suitable profile able to generate the SuperKamiokande spectrum.

We have also checked that combinations of real and imaginary parts for all couplings do not change the previous results. This should be expected since, as mentioned earlier, purely real couplings do not change the LMA probability. The only consequence of introducing real parts in the NSI couplings comes in the spectral event rates through the quantities $\tilde{g}_{L,R}$ in eqs.(14),(15), but the differences lie much beyond the experimental accuracy.

3.2 $(\varepsilon_{\alpha\beta}^{eP})_{CC} \neq (\varepsilon_{\alpha\beta}^{eP})_{NC}$

The analysis of the more general case of different CC and NC couplings affecting the $\nu_e e$ scattering diagrams can be made quite simple if one examines the coefficients of $(\varepsilon_{\alpha\beta}^{eP})_{CC}$ and $(\varepsilon_{\alpha\beta}^{eP})_{NC}$ in eq.(11). The first is unity whereas for equal CC and NC couplings it is 0.96 and the second is now -0.04 as compared to the previous value 0.96 as well. Consequently one expects that the analysis for $(\varepsilon_{\alpha\beta}^{eP})_{CC}$ leads to approximately the same results as for equal couplings while the results are modified by a factor of 0.96/(-0.04) in the analysis for $(\varepsilon_{\alpha\beta}^{eP})_{NC}$. Indeed the convenient modification in the LMA probability is obtained for

$$-i(|\varepsilon_{\mu\mu}^{eP}|)_{CC} = -i \, 1.4 \times 10^{-3} \quad (21)$$

or alternatively

$$+i(|\varepsilon_{\mu\mu}^{eP}|)_{NC} = +i \, 3.6 \times 10^{-2}. \quad (22)$$

which lead to the same probability as the cases listed in eq.(20). The results for the other couplings involving u and d quarks are of course unchanged. As before we have considered one coupling at a time to be non zero.

4 Conclusions

We have investigated the prospects for improving the LMA predictions for solar neutrino event rates with NSI. At present there is no evidence of any new physics associated to a scale not too far above the electroweak scale, hence the great variety of theoretical models available for NSI. In our approach we assumed that NSI are extra contributions to the vertices $\nu_\alpha \nu_\beta$ and $\nu_\alpha e$, so the new couplings describe the deviation from the standard model. With this in mind we derived the neutrino interaction potential in solar matter which was added to the standard Hamiltonian, proceeding with the integration of the evolution equation through the

Runge-Kutta method. Neutral and charged current couplings are involved in interactions with electrons whereas only neutral couplings affect those with quarks. We considered the new interactions both at the propagation and at the detection level. The improvement we searched for the LMA predictions consisted in finding whether and how the modification induced by NSI can lead to a flat spectral event rate for SuperKamiokande and an event rate for the CI experiment within 1σ of the data, while keeping the accuracy of all other predictions.

We used the current notation for the NSI couplings $\varepsilon_{\alpha\beta}^{e,u,d P}$ where α, β are the neutrino labels and e, u, d denote the charged fermion involved in the process. We investigated the range $|\varepsilon_{\alpha\beta}| \in [5 \times 10^{-5}, 5 \times 10^{-2}]$ and may summarize our main results as follows

- Real couplings $\varepsilon_{\alpha\beta}^{e,u,d P} = \pm |\varepsilon_{\alpha\beta}^{e,u,d P}|$ do not change the LMA probability when considered either one at a time or altogether and thus they induce a small change in the neutrino electron scattering rate ($\lesssim 1\%$) which is far beyond experimental visibility.
- Off diagonal couplings $\varepsilon_{\alpha\beta}^{e,u,d P}$ ($\alpha \neq \beta$) considered either one at a time or altogether do not change the LMA probability and thus the rates in a significant way.
- Diagonal, imaginary couplings $\varepsilon_{\alpha\alpha}^{e,u,d P} = \pm i |\varepsilon_{\alpha\alpha}^{e,u,d P}|$ are the only ones that lead to changes of all kinds in the probability and hence the rates.
- The couplings that lead to the 'best' results in the sense of leading to a flat spectral SuperKamiokande rate and a good fit for all other rates are as follows

$$\begin{aligned} -i|\varepsilon_{\mu\mu}^e P| &= -i 1.5 \times 10^{-3} \\ -i|\varepsilon_{\mu\mu}^u P| &= -i 2.5 \times 10^{-3} \\ +i|\varepsilon_{\mu\mu}^d P| &= +i 2.0 \times 10^{-3} \end{aligned} \quad (23)$$

within the assumption of equal charged (CC) and neutral current (NC) couplings.

- If one assumes different (CC) and (NC) couplings we have

$$\begin{aligned} -i(|\varepsilon_{\mu\mu}^e P|)_{CC} &= -i 1.4 \times 10^{-3} \\ +i(|\varepsilon_{\mu\mu}^e P|)_{NC} &= +i 3.6 \times 10^{-2}. \end{aligned} \quad (24)$$

In both cases (23) and (24) the results should be taken alternatively.

Since real couplings do not change the LMA probability, the insertion of real parts in the couplings does not lead to any change in the above results. We also note that whereas an increase in $\sin\theta_{13}$ leads to a mere decrease in the 8B spectral rate which translates in a parallel shift of the curve [27], a convenient choice of NSI couplings [eqs.(23) or (24)] induces in contrast an increased flatness. The situation is similar to the magnetic moment conversion to sterile neutrinos [27].

Unless stated otherwise our analyses were done for one coupling at a time. There are of course infinite combinations of couplings so that a complete investigation is not possible

and would unlikely lead to new conclusions. The aim of this paper is to prove that NSI provide a true possibility to solve the remaining inconsistencies within the solar neutrino problem.

Acknowledgements

We are grateful to Marco Picariello for useful discussions. C. R. Das gratefully acknowledges a scholarship from Fundação para a Ciência e Tecnologia ref. SFRH/BPD/41091/2007.

References

- [1] M. M. Guzzo, A. Masiero and S. T. Petcov, Phys. Lett. B **260** (1991) 154.
- [2] E. Roulet, Phys. Rev. D **44** (1991) 935.
- [3] Y. Grossman, Phys. Lett. B **359**, 141 (1995) [arXiv:hep-ph/9507344].
- [4] L. M. Johnson and D. W. McKay, Phys. Rev. D **61** (2000) 113007 [arXiv:hep-ph/9909355].
- [5] A. Datta, R. Gandhi, B. Mukhopadhyaya and P. Mehta, Phys. Rev. D **64**, 015011 (2001) [arXiv:hep-ph/0011375].
- [6] P. Huber and J. W. F. Valle, Phys. Lett. B **523**, 151 (2001) [arXiv:hep-ph/0108193].
- [7] P. Huber, T. Schwetz and J. W. F. Valle, Phys. Rev. Lett. **88**, 101804 (2002) [arXiv:hep-ph/0111224].
- [8] T. Ota, J. Sato and N. a. Yamashita, Phys. Rev. D **65** (2002) 093015 [arXiv:hep-ph/0112329].
- [9] P. Huber, T. Schwetz and J. W. F. Valle, Phys. Rev. D **66**, 013006 (2002) [arXiv:hep-ph/0202048].
- [10] S. Davidson, C. Pena-Garay, N. Rius and A. Santamaria, JHEP **0303**, 011 (2003) [arXiv:hep-ph/0302093].
- [11] J. Barranco, O. G. Miranda, C. A. Moura and J. W. F. Valle, Phys. Rev. D **73** (2006) 113001 [arXiv:hep-ph/0512195].
- [12] G. Mangano, G. Miele, S. Pastor, T. Pinto, O. Pisanti and P. D. Serpico, Nucl. Phys. B **756**, 100 (2006) [arXiv:hep-ph/0607267].

- [13] S. Antusch, J. P. Baumann and E. Fernandez-Martinez, Nucl. Phys. B **810**, 369 (2009) [arXiv:0807.1003 [hep-ph]].
- [14] C. Biggio, M. Blennow and E. Fernandez-Martinez, JHEP **0903**, 139 (2009) [arXiv:0902.0607 [hep-ph]].
- [15] A. M. Gago, H. Minakata, H. Nunokawa, S. Uchinami and R. Zukanovich Funchal, JHEP **1001**, 049 (2010) [arXiv:0904.3360 [hep-ph]].
- [16] C. Biggio, M. Blennow and E. Fernandez-Martinez, JHEP **0908**, 090 (2009) [arXiv:0907.0097 [hep-ph]].
- [17] C. Wei, arXiv:1003.1468 [hep-ph].
- [18] A. Esteban-Pretel, R. Tomas and J. W. F. Valle, Phys. Rev. D **76**, 053001 (2007) [arXiv:0704.0032 [hep-ph]].
- [19] Z. Berezhiani, R. S. Raghavan and A. Rossi, Nucl. Phys. B **638** (2002) 62 [arXiv:hep-ph/0111138].
- [20] A. Friedland, C. Lunardini and C. Pena-Garay, Phys. Lett. B **594** (2004) 347 [arXiv:hep-ph/0402266].
- [21] M. M. Guzzo, P. C. de Holanda and O. L. G. Peres, Phys. Lett. B **591** (2004) 1 [arXiv:hep-ph/0403134].
- [22] O. G. Miranda, M. A. Tortola and J. W. F. Valle, JHEP **0610** (2006) 008 [arXiv:hep-ph/0406280].
- [23] A. Bolanos, O. G. Miranda, A. Palazzo, M. A. Tortola and J. W. F. Valle, Phys. Rev. D **79** (2009) 113012 [arXiv:0812.4417 [hep-ph]].
- [24] F. J. Escrihuela, O. G. Miranda, M. A. Tortola and J. W. F. Valle, Phys. Rev. D **80** (2009) 105009 [Erratum-ibid. D **80** (2009) 129908] [arXiv:0907.2630 [hep-ph]].
- [25] G. L. Fogli *et al.*, Phys. Rev. D **78** (2008) 033010 [arXiv:0805.2517 [hep-ph]].
- [26] T. Schwetz, M. A. Tortola and J. W. F. Valle, New J. Phys. **10** (2008) 113011 [arXiv:0808.2016 [hep-ph]].
- [27] C. R. Das, J. Pulido and M. Picariello, Phys. Rev. D **79** (2009) 073010 [arXiv:0902.1310 [hep-ph]].
- [28] J. Pulido, C. R. Das and M. Picariello, J. Phys. Conf. Ser. **203** (2010) 012086 [arXiv:0910.0203 [hep-ph]].

- [29] S. Fukuda *et al.* [Super-Kamiokande Collaboration], Phys. Lett. B **539**, 179 (2002) [arXiv:hep-ex/0205075].
- [30] J. P. Cravens *et al.* [Super-Kamiokande Collaboration], Phys. Rev. D **78**, 032002 (2008) [arXiv:0803.4312 [hep-ex]].
- [31] Contribution to TAUP 2009, Rome July 1-5, 2009, <http://www.iop.org/EJ/toc/1742-6596/203/1>.
- [32] B. T. Cleveland *et al.*, Astrophys. J. **496** (1998) 505.
- [33] P. C. de Holanda and A. Y. Smirnov, Phys. Rev. D **69** (2004) 113002 [arXiv:hep-ph/0307266].
- [34] D. Aristizabal Sierra, M. Hirsch and S. G. Kovalenko, Phys. Rev. D **77** (2008) 055011 [arXiv:0710.5699 [hep-ph]].
- [35] M. Malinsky, J. C. Romao and J. W. F. Valle, Phys. Rev. Lett. **95** (2005) 161801 [arXiv:hep-ph/0506296].
- [36] F. Bazzocchi, D. G. Cerdeno, C. Munoz and J. W. F. Valle, arXiv:0907.1262 [hep-ph].
- [37] M. Malinsky, T. Ohlsson and H. Zhang, Phys. Rev. D **79** (2009) 011301 [arXiv:0811.3346 [hep-ph]].
- [38] Z. Berezhiani and A. Rossi, Phys. Lett. B **535** (2002) 207 [arXiv:hep-ph/0111137].
- [39] M. B. Gavela, D. Hernandez, T. Ota and W. Winter, Phys. Rev. D **79** (2009) 013007 [arXiv:0809.3451 [hep-ph]].
- [40] C. Pena-Garay and A. Serenelli, arXiv:0811.2424 [astro-ph].
- [41] Z. Maki, M. Nakagawa and S. Sakata, Prog. Theor. Phys. **28** (1962) 870.
- [42] C. Amsler *et al.* [Particle Data Group], Phys. Lett. B **667**, 1 (2008).
- [43] Y. Fukuda *et al.* [Super-Kamiokande Collaboration], Phys. Rev. Lett. **81**, 1158 (1998) [Erratum-ibid. **81**, 4279 (1998)] [arXiv:hep-ex/9805021].
- [44] B. Aharmim *et al.* [SNO Collaboration], Phys. Rev. C **72** (2005) 055502 [arXiv:nucl-ex/0502021].
- [45] C. Cattadori, N. Ferrari and L. Pandola, Nucl. Phys. Proc. Suppl. **143** (2005) 3.
- [46] V. N. Gavrin and B. T. Cleveland, arXiv:nucl-ex/0703012.
- [47] B. Aharmim *et al.* [SNO Collaboration], arXiv:0910.2984 [nucl-ex].

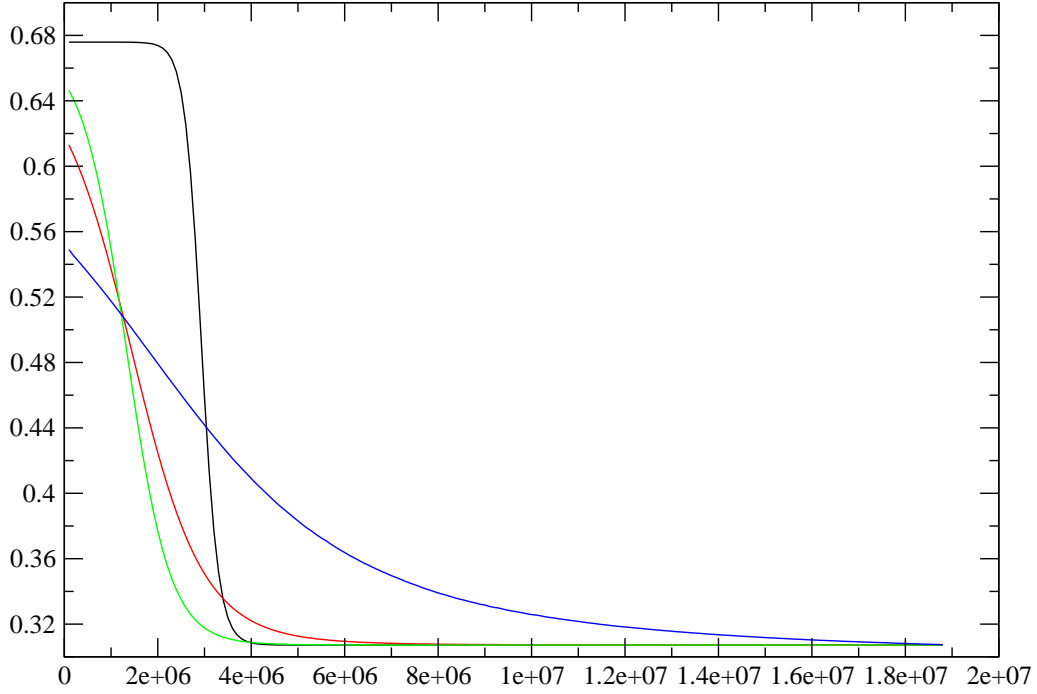


Figure 1: *Survival probabilities as a function of neutrino energy in eV. At the lowest energy and from bottom to top, the first curve is the LMA one, the next is the one providing the best fit to the data with $-i|\varepsilon_{\mu\mu}^e{}^P| = -i 1.5 \times 10^{-3}$ [eq.(20)], the next is for $-i|\varepsilon_{\mu\mu}^e{}^P| = -i 3 \times 10^{-3}$ and the top one is for $-i|\varepsilon_{\mu\mu}^e{}^P| = +i 5 \times 10^{-3}$ with other non standard couplings vanishing in each case. The last two curves lead to an unacceptably high Ga rate prediction [45, 46].*

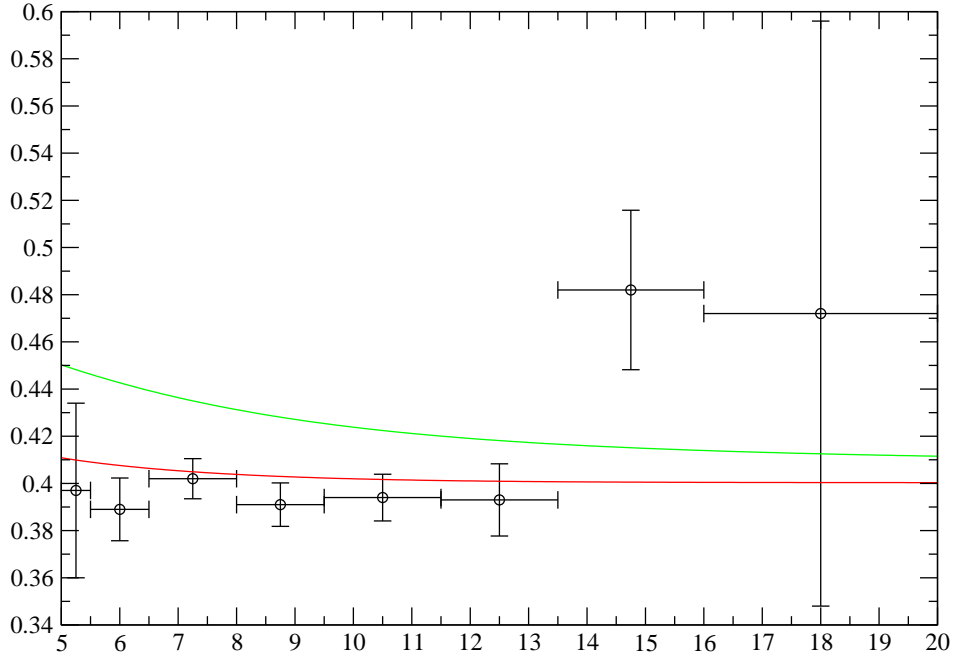


Figure 2: *Predictions for SuperKamiokande (units in MeV for electron energy). The upper curve is the LMA spectrum and the lower curve is the LMA spectrum with non standard interactions as in eqs.(23) or (24). These are superimposed on the data published by the Collaboration in 2002 [29].*

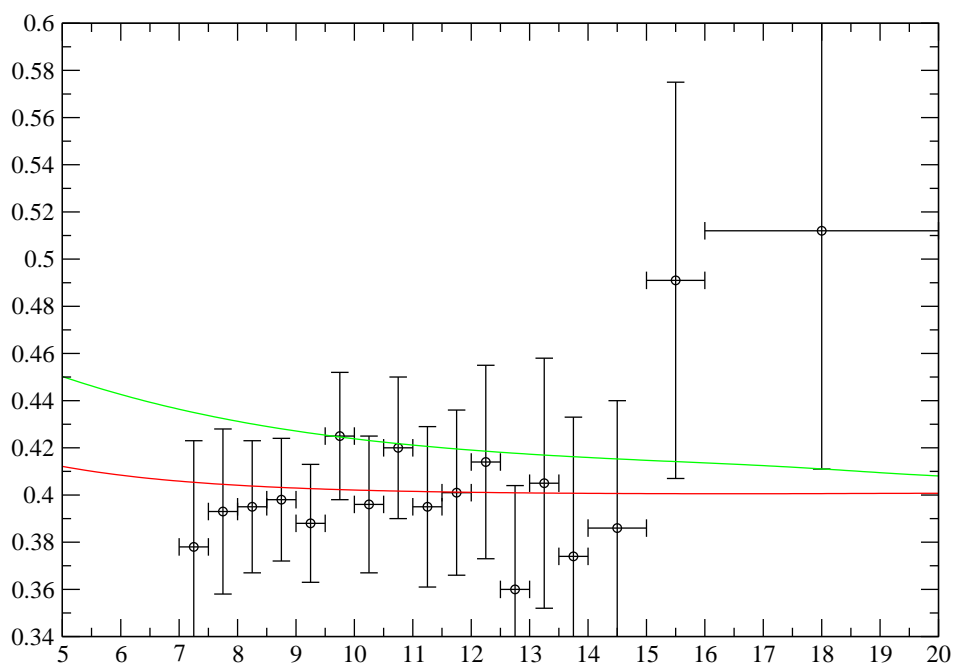


Figure 3: *Same as fig.2 with the data published in 2008 [30].*

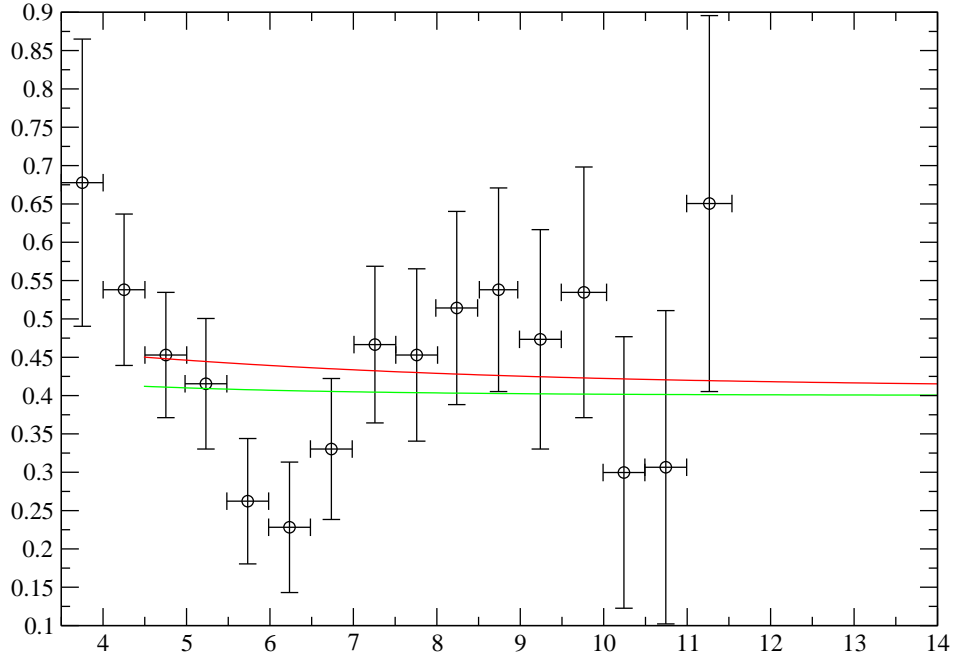


Figure 4: *Predictions for SNO neutrino electron scattering superimposed on the data [47] (units in MeV for electron kinetic energy). The upper curve is the LMA prediction and the lower curve is the LMA one with non standard interactions. Errors bars are larger than in SuperKamiokande so that the data are consistent with a flat spectrum.*